



HAL
open science

Quantification of the effects of vasomotion on mass transport to tissue from axisymmetric blood vessels

Tharindi Hapuarachchi, Chang Sub Park, Stephen Payne

► **To cite this version:**

Tharindi Hapuarachchi, Chang Sub Park, Stephen Payne. Quantification of the effects of vasomotion on mass transport to tissue from axisymmetric blood vessels. *Journal of Theoretical Biology*, 2010, 264 (2), pp.553. 10.1016/j.jtbi.2010.03.002 . hal-00585806

HAL Id: hal-00585806

<https://hal.science/hal-00585806>

Submitted on 14 Apr 2011

HAL is a multi-disciplinary open access archive for the deposit and dissemination of scientific research documents, whether they are published or not. The documents may come from teaching and research institutions in France or abroad, or from public or private research centers.

L'archive ouverte pluridisciplinaire **HAL**, est destinée au dépôt et à la diffusion de documents scientifiques de niveau recherche, publiés ou non, émanant des établissements d'enseignement et de recherche français ou étrangers, des laboratoires publics ou privés.

Author's Accepted Manuscript

Quantification of the effects of vasomotion on mass transport to tissue from axisymmetric blood vessels

Tharindi Hapuarachchi, Chang Sub Park, Stephen Payne

PII: S0022-5193(10)00125-6
DOI: doi:10.1016/j.jtbi.2010.03.002
Reference: YJTBI5903



www.elsevier.com/locate/jtbi

To appear in: *Journal of Theoretical Biology*

Received date: 27 August 2009
Revised date: 1 March 2010
Accepted date: 1 March 2010

Cite this article as: Tharindi Hapuarachchi, Chang Sub Park and Stephen Payne, Quantification of the effects of vasomotion on mass transport to tissue from axisymmetric blood vessels, *Journal of Theoretical Biology*, doi:[10.1016/j.jtbi.2010.03.002](https://doi.org/10.1016/j.jtbi.2010.03.002)

This is a PDF file of an unedited manuscript that has been accepted for publication. As a service to our customers we are providing this early version of the manuscript. The manuscript will undergo copyediting, typesetting, and review of the resulting galley proof before it is published in its final citable form. Please note that during the production process errors may be discovered which could affect the content, and all legal disclaimers that apply to the journal pertain.

Quantification of the effects of vasomotion on mass transport to tissue from axisymmetric blood vessels

Tharindi Hapuarachchi¹, Chang Sub Park and Stephen Payne²

Institute of Biomedical Engineering, Department of Engineering Science, University of Oxford,
Parks Road, Oxford OX1 3PJ, UK

t.hapuarachchi@ucl.ac.uk, chang.park@eng.ox.ac.uk, stephen.payne@eng.ox.ac.uk

Abstract

The process known as vasomotion, rhythmic oscillations in vessel diameter, has been proposed to act as a protective mechanism for tissue under conditions of reduced perfusion, since it is frequently only observed experimentally when perfusion levels are reduced. This could be due to a resultant increase in oxygen transport from the vasculature to the surrounding tissue, either directly or indirectly. It is thus potentially of significant clinical interest as a warning signal for ischemia. However, there has been little analysis performed to quantify the effects of vessel wall movement on time-averaged mass transport. We thus present a detailed analysis of such mass transport for an axisymmetric vessel with a periodically oscillating wall, by solving the non-linear mass transport equation, and quantify the differences between the time-averaged mass transport under conditions of no oscillation (i.e. the steady-state) and varying wall oscillation amplitude. The results show that if the vessel wall alone is oscillated, with an invariant wall concentration, the time-averaged mass transport is reduced relative to the steady-state, but if the vessel wall concentration is also oscillated, then mass transport is increased, although this is generally only true when these oscillate in phase with each other. The influence of Péclet number and the non-

¹ This work was performed in Oxford as part of a Wellcome Trust Biomedical Vacation Scholarship.

² Corresponding author: tel: 01865 617656; fax: 01865 617702; email: stephen.payne@eng.ox.ac.uk

dimensional rate of consumption of oxygen in tissue, as well as the amplitude of oscillations, are fully characterised. We conclude by considering the likely implications of these results in the context of oxygen transport to tissue.

Keywords: Oscillations; Ischemia; Non-linear dynamics

1 Introduction

Vasomotion is the process of oscillation in vascular tone, generated from within the vessel wall. Although it has been seen in many studies over many years, the physiological consequences of vasomotion remain very unclear, Nilsson and Aalkjaer, 2003. One potential benefit is that the time-averaged hydraulic resistance to flow is lower than the steady state resistance, due to the non-linear relationship between vessel radius and resistance, Meyer et al., 2002. Another hypothesis is that it improves tissue oxygenation, Tsai and Intaglietta, 1993, although this is controversial, Goldman and Popel, 2001. Experimental studies have shown that as perfusion levels are reduced, vasomotion is induced in most muscle preparations, Rucker et al., 2000. There is thus the possibility that vasomotion is induced under conditions of reduced perfusion as a protective mechanism against ischemia.

The equations governing mass transport to tissue, outlined below, are strongly non-linear (as is the equation relating flow to vessel diameter). A temporal oscillation of the vessel diameter about its steady-state value will cause the time-averaged behaviour to differ from the steady-state behaviour, possibly quite significantly at high oscillation amplitudes. However, solutions to these equations thus have to be considered carefully to ensure that the oscillating concentration profile in the tissue is characterised accurately. We present below a novel technique to solve for this concentration profile in the full non-linear case for a periodically oscillating wall diameter. This enables us to calculate the unsteady mass transport and hence to quantify the effects of vasomotion on the time-averaged mass transfer from individual vessels. We then conclude by

discussing the potential implications of this for our understanding of the physiological role of vasomotion.

2 Theory

2.1 Concentration equation

We start from the general mass transport equation for the concentration of gas in the tissue surrounding a blood vessel:

$$\frac{\partial C}{\partial t} + U \cdot \nabla C = D \nabla^2 C - R, \quad (1)$$

where C is the concentration of gas dissolved in the tissue, U is the velocity field of the tissue, D is the diffusion coefficient of gas in the tissue and R is the rate of reaction (assumed negative here since the gas in question here, oxygen, is metabolised and hence essentially continuously removed from the tissue). For an axisymmetric vessel in cylindrical co-ordinates, assuming a rate of reaction linearly proportional to the concentration of gas in the tissue, this becomes:

$$\frac{\partial C}{\partial t} + \frac{R(t)R(r)}{r} \frac{\partial C}{\partial r} = \frac{D}{r^2} \frac{\partial}{\partial r} \left[r^2 \frac{\partial C}{\partial r} \right] - kC, \quad (2)$$

where r is the radial coordinate measured from the centre of the vessel, R is the radius of the vessel (explicitly given as a function of time) and k is the metabolic rate constant. The assumptions made here will be discussed in full detail below in the context of the results. Note that the second term in equation 2, which introduces the non-linearity into the model, is derived from continuity considerations for the tissue surrounding the vessel.

Equation 2 is then re-cast in non-dimensional form, with respect to a length scale R_0 , a timescale T and the angular frequency of oscillation ω :

$$\xi = \frac{r}{R_0}, \quad x = \frac{R}{R_0}, \quad \tau = \frac{t}{T}, \quad K = \frac{k}{\omega}, \quad (3)$$

to give:

$$\frac{\partial C}{\partial \tau} + \frac{x(\tau)k(\tau)\partial C}{\xi} = \frac{1}{Pe} \frac{\partial}{\partial \xi} \left[\xi^2 \frac{\partial C}{\partial \xi} \right] - KC, \quad (4)$$

where $Pe = R_0^2/DT$ is the Péclet number and $\omega T = 1$, without loss of generality.

Using a similar approach to that of Fyrrillas and Szeri, 1994, equation 4 is re-written in Lagrangian

coordinates, where $\sigma = \frac{\xi^2 - x^2}{2}$:

$$\frac{\partial C}{\partial \tau} = \frac{1}{Pe} \frac{\partial}{\partial \sigma} \left[\frac{(2\sigma + x^2)\partial C}{\partial \sigma} \right] - KC, \quad (5)$$

with boundary conditions:

$$C(\sigma = 0, \tau) = C_w(\tau), \quad (6a)$$

$$C(\sigma \rightarrow \infty, \tau) \rightarrow 0, \quad (6b)$$

where C_w is the (possibly temporally varying) concentration of gas in the liquid at the wall. This is of course governed by the flow and transport conditions inside the vessel, but for now is specified independently. The second boundary condition assumes an infinitely far off boundary, which assumes that the vessel being modelled is independent of all other vessels. The likely impact of this on the solution will be discussed later. Note that the consumption rate constant is assumed to be invariant with space, without an explicit separate treatment of the vessel wall: this is based on the findings of Sharan et al., 2008, where the metabolic rate of oxygen was shown to be the same in the vessel wall as for the surrounding tissue.

A periodically oscillating boundary displacement is imposed:

$$x(\tau) = 1 + \varepsilon e^{i\tau} + \varepsilon^* e^{-i\tau}, \quad (7)$$

where $\varepsilon, \varepsilon^*$ are arbitrary complex conjugates, the magnitude of which are proportional to the amplitude of oscillations. Given the periodic nature of the wall movement, once any initial transients have died away, the gas concentration at each point in space will also be periodic in nature. This allows a separation of variables to be made for the concentration profile:

$$C(\sigma, \tau) = \sum_{n=-N}^N C_n(\sigma) e^{in\tau}, \quad (8)$$

where $C_{-n}(\sigma) = C_n^*(\sigma)$ and $C_n(\sigma), C_n^*(\sigma)$ are complex conjugates. Note that a full Fourier series is used here to arbitrary order of n , as is required due to the non-linear nature of the governing equations. Such a series could also be used for the wall displacement if required, although only the lowest harmonics are likely to be significant in either expansion.

Substituting the above in equation (5) gives:

$$\sum_{n=-N}^N C_n in \varepsilon^{in\tau} = \frac{1}{P\varepsilon} \sum_{n=-N}^N \left[(2\sigma + (1 + \varepsilon e^{i\tau} + \varepsilon^* e^{-i\tau})^2) \frac{d^2 C_n}{d\sigma^2} + 2 \frac{dC_n}{d\sigma} \right] e^{in\tau} - K \sum_{n=-N}^N C_n e^{in\tau}. \quad (9)$$

The terms in equation (9) corresponding to the 0th and 1st harmonics must individually balance. We assume at this point that the 2nd harmonic terms are negligible in comparison with the 0th and 1st harmonics, since the process is being driven by a wall movement containing only a fundamental component. It would, of course, be possible to map out all the harmonic terms in the solution by balancing up to arbitrary order in equation 9 but we do not do this here. Balancing the 0th, 1st and -1st harmonic terms thus gives:

$$0 = (2\sigma + 1 + 2\varepsilon\varepsilon^*) \frac{d^2 C_0}{d\sigma^2} + 2 \frac{dC_0}{d\sigma} + 2\varepsilon \frac{d^2 C_1^*}{d\sigma^2} + 2\varepsilon^* \frac{d^2 C_1}{d\sigma^2} - KP\varepsilon C_0, \quad (10)$$

$$iP\epsilon C_1 = (2\sigma + 1 + 2\epsilon\epsilon^*) \frac{d^2 C_1}{d\sigma^2} + 2 \frac{dC_1}{d\sigma} + 2\epsilon \frac{d^2 C_0}{d\sigma^2} - KP\epsilon C_1, \quad (11)$$

$$-iP\epsilon C_1^* = (2\sigma + 1 + 2\epsilon\epsilon^*) \frac{d^2 C_1^*}{d\sigma^2} + 2 \frac{dC_1^*}{d\sigma} + 2\epsilon^* \frac{d^2 C_0}{d\sigma^2} - KP\epsilon C_1^*. \quad (12)$$

To simplify the solution, we re-write the coefficients in real and imaginary parts, such that $\epsilon = a + ib$, $C_1(\sigma) = \alpha_1(\sigma) + i\beta_1(\sigma)$, where a and b govern the magnitude and phase of the imposed boundary oscillation. Equations (10), (11) and (12) then reduce to:

$$(2\sigma + 1 + 2(a^2 + b^2)) \frac{d^2 C_0}{d\sigma^2} + 2 \frac{dC_0}{d\sigma} + 4a \frac{d^2 \alpha_1}{d\sigma^2} + 4b \frac{d^2 \beta_1}{d\sigma^2} - KP\epsilon C_0 = 0, \quad (13)$$

$$(2\sigma + 1 + 2(a^2 + b^2)) \frac{d^2 \alpha_1}{d\sigma^2} + 2 \frac{d\alpha_1}{d\sigma} - KP\epsilon \alpha_1 + 2a \frac{d^2 C_0}{d\sigma^2} + P\epsilon \beta_1 = 0, \quad (14)$$

$$(2\sigma + 1 + 2(a^2 + b^2)) \frac{d^2 \beta_1}{d\sigma^2} + 2 \frac{d\beta_1}{d\sigma} - KP\epsilon \beta_1 + 2b \frac{d^2 C_0}{d\sigma^2} - P\epsilon \alpha_1 = 0. \quad (15)$$

The complexity of these three coupled equations prevents an analytical solution from being derived. The presence of an infinitely far away boundary then also makes imposing suitable boundary conditions numerically difficult. To overcome this problem by converting the problem into a bounded co-ordinate system, equations (13), (14) and (15) are re-written using the co-ordinate transformation $s = \frac{1}{1 + 2\sigma}$:

$$(4s^3 + 8s^4(a^2 + b^2)) \frac{d^2 C_0}{ds^2} + (4s^1(23 - 22s) \frac{dC_0}{ds} - KP\epsilon C_0 = 0,$$

$$(4s^3 + 8s^4(a^2 + b^2)) \frac{d^2 \alpha_1}{ds^2} + (4s^1(23 - 22s) \frac{d\alpha_1}{ds} - KP\epsilon \alpha_1 + 2a \frac{d^2 C_0}{ds^2} + P\epsilon \beta_1 = 0,$$

$$(4s^3 + 8s^4(a^2 + b^2)) \frac{d^2 \beta_1}{ds^2} + (4s^1(23 - 22s) \frac{d\beta_1}{ds} - KP\epsilon \beta_1 + 2b \frac{d^2 C_0}{ds^2} - P\epsilon \alpha_1 = 0.$$

Note that the problem now reduces to 3 simple 2nd order differential equations that can easily be solved numerically within the range $0 < s < 1$ ($s = 0$ corresponding to the tissue infinitely far

away from the vessel and $s = 1$ corresponding to the vessel wall). The boundary conditions are set by the particular nature of the problem under investigation, as discussed below.

Note that in the steady state, equation (16) reduces to:

$$4s^2 \frac{d^2 [C_1]_{ss}}{ds^2} + 4s \frac{d[C_1]_{ss}}{ds} = 0$$

which can again easily be solved with the same boundary conditions, enabling a direct comparison to be made with the oscillating solution.

2.2 Mass transport equation

Before examining the solutions to the concentration equations, we examine the mass transport equation, since the aim is to compare the rate of mass transfer from vessel to tissue under oscillating and non-oscillating conditions. The rate of diffusive mass transport of gas across the wall is given by:

$$\dot{m} = -D_w 2\pi R \left. \frac{\partial C}{\partial r} \right|_{r=R} \quad (20)$$

where D_w is the diffusion coefficient of gas through the wall. In Lagrangian coordinates:

$$\dot{m} = -D_w 2\pi R_0 x^2 \left. \frac{\partial C}{\partial \sigma} \right|_{\sigma=0} \quad (21)$$

Substitution of equations (7) and (8) and transformation into the bounded coordinate system yields:

$$\dot{m}_{\text{cs}} = -D_w 4\pi R_0 \left[(1 + 2\alpha^2) \left. \frac{dC_0}{ds} \right|_{s=1} + 4\alpha \left. \frac{d\alpha_1}{ds} \right|_{s=1} \right] \quad (22)$$

for the time averaged mass transport. Note that the oscillating mass transport component is ignored here since it makes no contribution to the net mass transport from blood to tissue.

In the steady state the rate of mass transport is given by:

$$\dot{m}_{ss} = -D_w 4\pi R_0 \left. \frac{dC_{0,ss}}{ds} \right|_{s=1}, \quad (23)$$

where this is calculated directly from the solution to equation (19). Note that the expression for

$\frac{dC_{0,ss}}{ds}$ is not the same as the expression for $\frac{dC_0}{ds}$ in equation (22). This is due to the non-linearities in the system affecting the time-averaged mass transport as described previously. The ratio of time-averaged mass transport to steady state mass transport is then:

$$\frac{\dot{m}_{ta}}{\dot{m}_{ss}} = \frac{(1 + 2\alpha^2) \left. \frac{dC_0}{ds} \right|_{s=1} + 4\alpha \left. \frac{d\alpha_1}{ds} \right|_{s=1}}{\left. \frac{dC_{0,ss}}{ds} \right|_{s=1}}, \quad (24)$$

which we term the Mass Transport Ratio. It is this ratio that is of primary interest here.

3 Results

Two sets of solutions are considered here. In the first set, the wall is oscillated but the wall concentration is kept constant. The boundary conditions thus become:

$$s = 0: \quad C_0 = \frac{d\alpha_1}{ds} = \frac{d\beta_1}{ds} = 0, \quad (25a)$$

$$s = 1: \quad C_0 = C_w; \quad \alpha_1 = \beta_1 = 0. \quad (25b)$$

In the second, both the wall and the wall concentration are oscillated. The boundary conditions then become:

$$s = 0: \quad C_0 = \frac{d\alpha_1}{ds} = \frac{d\beta_1}{ds} = 0, \quad (26a)$$

$$s = 1: \quad C_0 = C_w; \quad \alpha_1 = \alpha_0; \quad \beta_1 = \beta_0. \quad (26b)$$

α_0 and β_0 are set by the magnitude and phase of the wall concentration oscillations, relative to the wall displacement. For all the simulations presented below, the governing equations were solved with the specified boundary conditions using the Matlab solver, `bvp4c`. From the complete solution for the concentration profile, the wall concentration gradients in equation (24) were then estimated numerically.

Since the absolute phase of the solutions is arbitrary, we set $b=0$ without loss of generality. Equation (7) then simplifies to $x = 1 + 2a \cos(\tau)$. The wall displacement oscillations are thus defined to be the reference phase, relative to which are measured the concentration oscillations. Note that the results are only dependent on the values of two non-dimensional parameters (Péclet number and non-dimensional rate constant) and the amplitude of the wall displacement ($2a$) and amplitude and phase of the wall concentration (α_0 and β_0) oscillations.

To illustrate the model predictions, the results for $C_{0,s}$, α_1 and β_1 are shown against the co-ordinate s for the condition where $K = 1$, $a = 0.2$ and $Pe = 0.1$ in Figure 1. Despite the fact that the oscillating components are constrained to be zero at both ends of the co-ordinate system and to have zero gradient at the outer boundary ($s = 0$), there is a non-zero gradient at the inner boundary ($s = 1$), which is what alters the time-averaged mass transport from that in the steady state (equation 24). Note that the gradient for α_1 is negative, which is why the time-averaged mass transport is lower than in the steady state.

3.1 Wall displacement oscillation only

We first consider the effects of oscillating only the wall displacement. Figure 2 shows the effect of vasomotion on the Mass Transport Ratio at different values of the Péclet number for a fixed value of $K = 1$ and a range of wall amplitudes, $a < 0.5$. For all solutions, as the wall amplitude tends towards zero, the mass transfer ratio tends towards 1, as expected, since the governing equations

become linear in the limit. As a increases, however, this ratio decreases monotonically: at low amplitudes of oscillation, the effect of Péclet number is small, but at amplitudes greater than approximately $a > 0.25$, decreases in Péclet number result in a reduction in mass transfer ratio.

For an increased value of $K = 10$, the results are very similar, Figure 3. The mass transfer ratio is slightly higher than for $K = 1$, but the difference is only slight. For a decreased value of K , as shown in Figure 4, the results are likewise rather insensitive to the precise value of K apart from at high values of Péclet number, where there is a slight increase in the time-averaged mass transport. The mass transport ratio, however, is uniformly less than 1 for all the values considered here, indicating that the oscillation in wall displacement causes a reduction in mass transfer over all ranges of parameter values investigated.

3.2 Wall displacement and wall concentration oscillations

We next consider the case where the wall concentration also oscillates. Four cases are shown in Figures 5-8, considering the cases where the amplitude of concentration oscillation is 0.5: Figure 5, in phase with the wall displacement ($\alpha_0 = 0.5$, $\beta_0 = 0$); Figure 6, 90 degrees ahead ($\alpha_0 = 0$, $\beta_0 = 0.5$); Figure 7, 180 degrees out of phase ($\alpha_0 = -0.5$, $\beta_0 = 0$); Figure 8, 90 degrees behind ($\alpha_0 = 0$, $\beta_0 = -0.5$). In all cases the value of K was kept constant ($K = 1$).

The interaction between wall displacement and wall concentration oscillations is clearly substantially more complicated than for wall displacement oscillations alone. Under most conditions, the mass transport reduces, but there are some cases when this mass transport increases, potentially very significantly.

When the wall displacement and wall concentration oscillations are in phase, at Péclet numbers greater than about 1, the mass transport is found to increase over all values of a . However, for Péclet numbers smaller than this, the ratio is less than 1, indicating a drop in mass transport.

When the concentration oscillates 90 degrees ahead, the mass transport is lower under virtually all combinations of Péclet number and displacement amplitude: only for moderate amplitudes and very low values of Péclet number is the mass transport enhanced, and this is a small effect.

Similar results are found for a 180 degree phase shift: only at moderate amplitudes of displacement oscillation and very low Péclet number does the mass transport increase, and again only fractionally. The results for a 90 degrees phase shift behind, however, are quite substantially different. For low values of Péclet number, the mass transport decreases over all values of α , but for values greater than approximately $Pe = 1$, there is a moderate increase in mass transport over a wide range of α .

4 Discussion

The results presented above show that the time-averaged mass transport is very significantly different from the steady-state mass transport under a wide range of conditions. We now consider the typical values of the non-dimensional parameters found in the vasculature before examining the accuracy and potential physiological implications of the results obtained here.

The diffusion coefficient of oxygen in tissue, D , has been measured at 37 °C to be $2.4 \times 10^{-9} \text{ m}^2/\text{s}$ (Bentley et al., 1993) and this value is used throughout. The metabolic rate constant is more complicated, as the linear consumption equation used here is only an approximation to the complex underlying metabolic processes. We provide a first order estimate by dividing the metabolic rate of oxygen by the typical concentration of oxygen in the tissue. The former is quoted as $8.2 \times 10^{-4} \text{ cm}^3\text{O}_2/\text{cm}^3/\text{s}$ and the latter as $2.6 \times 10^{-4} \text{ cm}^3\text{O}_2/\text{cm}^3$ (Mintun et al., 2001), yielding an approximate value for the rate constant of 3.2 /s. This is clearly a gross estimate for this parameter, but the fact that it is greater than 1 indicates (from the results presented earlier) that there is little sensitivity to its precise value. We note in passing that spatial measurements of

static oxygen partial pressure in tissue remain highly controversial and uncertain, see for example Golub et al., 2007, and Tsai et al., 1998, which makes evaluation of the metabolic rate constant from experimental data still difficult.

Colantuoni et al., 1984, measured the vasomotive activity in hamsters using image analysis techniques to capture the frequency and amplitude of oscillation of four types of arteriolar vessels (mean arteries, small arteries, arterioles and terminal arterioles). They found that the amplitude of oscillation increased with vessel radius as well as with frequency. The resulting values of Péclet number and non-dimensional rate constant are given in Table 1. Note that the Péclet number varies over nearly two orders of magnitude over the arterial network, since it is proportional to the square of the baseline vessel radius. K varies over a much smaller range, since the oscillation frequency is nearly invariance with radius. In the smallest vessels, vasomotion results in very large displacement amplitudes.

Rucker et al., 2000, measured the vasomotive activity in rats in both the transverse and terminal arterioles, with their experimental values yielding a Péclet number of approximately 0.02 (based on a diameter of 10 μm) and K of approximately 15. The amplitude of oscillation was found to be approximately 60 %, these values being in fairly good agreement with those of Colantuoni et al., 1984 (although the frequency of oscillation was found to be somewhat slower). Although these measurements were not made in humans, they are in good agreement for Péclet number with only a small (and irrelevant) difference in K .

Type of vessel	Mean radius (μm)	Oscillation frequency (cycles/min)	Amplitude of oscillation	Pe	K
Mean artery	85	2.74	19.3 %	0.864	11.2
Small artery	55.7	3.36	20.8 %	0.455	9.09

Arteriole	27.03	5.42	32.2 %	0.173	5.64
Terminal arteriole	7.05	9.47	89 %	0.0205	3.23

Table 1 Parameter values and non-dimensional quantities taken from Colantuoni et al., 1984

Geometrically it has been assumed that the vessel is axisymmetric in an infinite tissue. The assumption of an infinite volume of tissue surrounding each vessel is clearly inaccurate and is included here to reduce the number of parameters involved in the model. A Krogh style cylinder is often used in similar models, but the results can be sensitive to the particular choice of outer radius, which makes interpretation of the results difficult. However, the primary reason for choosing an infinite volume is the fact that the governing equation used here is linear in concentration. The actual tissue concentration can then be considered simply as the summation of the solutions for all individual vessels, each of which is surrounded by an infinite volume of tissue. Although this will have some inherent inaccuracies, as long as the vessels are reasonably well-spaced, it is likely that the mass transport from individual vessels will be well captured.

The other major assumption made here is that there are no axial variations in the concentration or displacement profiles, this being done since it reduces the computational requirement very substantially. We can however, estimate their effects by considering the effects of axial waves along the vessel (the possible cause of such waves will be considered later). The governing equation (2) becomes:

$$\frac{\partial C}{\partial t} + \frac{R(r)\dot{R}(r)}{r} \frac{\partial C}{\partial r} = \frac{D}{r^2} \frac{\partial}{\partial r} \left[r^2 \frac{\partial C}{\partial r} \right] + D \frac{\partial^2 C}{\partial z^2} - kC, \quad (27)$$

where z is the axial coordinate. In non-dimensional form, this becomes:

$$\frac{\partial C}{\partial \tau} + \frac{x(\tau)\dot{x}(\tau)}{\xi} \frac{\partial C}{\partial \xi} = \frac{1}{Pe} \frac{\partial}{\partial \xi} \left[\xi^2 \frac{\partial C}{\partial \xi} \right] + \frac{1}{Pe} \left(\frac{R_0}{l} \right)^2 \frac{\partial^2 C}{\partial \zeta^2} - KC, \quad (28)$$

where $\zeta = z/l$ is the non-dimensional axial coordinate and l is the characteristic length of the vessel. The trial solution for the concentration profile would be of the form:

$$C(\sigma, \zeta, \tau) = \sum_{n=-N}^N C_n(\sigma) e^{i(n\tau + \lambda \zeta)}, \quad (29)$$

where the non-dimensional wavelength of the axial waves is λ , this depending on the imposed form of the solution. The equivalent form of equation (9) is then:

$$\sum_{n=-N}^N C_n i n e^{i n \tau} = \frac{1}{Pe} \sum_{n=-N}^N \left[(2\sigma + (1 + e^{i n \tau} + e^{-i n \tau})) \frac{d^2 C_n}{d\sigma^2} + 2 \frac{dC_n}{d\sigma} \right] e^{i n \tau} - \left(K + \frac{\lambda^2}{Pe} \left(\frac{R_0}{l} \right)^2 \right) \sum_{n=-N}^N C_n e^{i n \tau}.$$

The only effect of imposing an axial wave-like behaviour is thus to increase the effective value of the non-dimensional metabolic rate constant from K to $K + \frac{\lambda^2}{Pe} \left(\frac{R_0}{l} \right)^2$. The general solution to equation 30 is otherwise unaffected. The effect of axial variations will thus depend upon both the absolute change in the effective value of K and the sensitivity of the solution to these changes. If it is assumed that the non-dimensional wavelength is of order 1 (i.e. the wavelength is the same order of magnitude as the vessel length) and that the vessel radius to length ratio is of order 0.1 (since most vessels are significantly longer than their radius), the increase in effective K is of order $0.01/Pe$. This will be greatest when the Péclet number is smallest, which occurs in the smallest vessels, where it is approximately 0.02, yielding an increase in effective K of less than 1. Since baseline K is around 3 and the results shown previously indicate that above a value of approximately 1, the precise value of K has little impact on the results, axial variations are likely to have only a second order impact on the mass transport.

Clearly, however, the model presented here has significant limitations in the assumption of a linear model for concentration and metabolism. This was done here simply to gain an insight into the previously unconsidered process of the dynamic interaction between wall displacement and

tissue concentration field by taking the form of the equation that provides a physiologically realistic concentration profile in the simplest mathematical form. It will be necessary in future to consider a more detailed model for oxygen tension and myoglobin saturation (as done in Goldman and Popel, 2001, for example) and to attempt to validate the static concentration field against experimental data, although this remains challenging, as previously discussed.

Although the values of model parameters can be estimated reasonably accurately from the experimental literature, direct validation of the results presented here is extremely difficult. Measurement of the dynamic oxygen concentration profile surrounding a vessel to the required order of accuracy is experimentally very challenging and no suitable data exist to the best of our knowledge. Measurement of the changes in time-averaged mass transport would appear only to be experimentally feasible by quantifying the changes in oxygen saturation of the blood exiting a vasomotive vessel or network to test whether this is higher under vasomotive conditions than under normal conditions. However, since vasomotion is normally induced by a reduction in perfusion, which will also directly lead to a substantive change in the oxygen saturation of the exiting blood, it is debatable whether such a reduction is capable of being measured accurately enough to provide a direct validation of the results presented in this paper.

There has been some debate in the literature about the role of vasomotion in promoting the supply of oxygen to tissue, particularly under conditions of reduced perfusion, when the supply would otherwise be expected to be reduced with severe consequences. The role of vasomotion as a protective mechanism was first proposed by Tsai and Intaglietta, 1993, where it was suggested that long-range oxygen diffusion was increased under such conditions, thus providing a protective mechanism for vulnerable tissue. This was re-examined by Goldman and Popel, 2001, where it was concluded that this was only the case at low myoglobin levels. Rucker et al., 2000, found experimentally that vasomotion promoted the supply of blood to adjacent tissues, which implies

that there are additional processes occurring during the conditions that induce vasomotion, which may not be directly related to the vasomotive process.

The vascular network is highly complex with vessels over a wide range of length scales and active autoregulatory processes affecting vessel diameters across the network (particularly in the arteriolar bed) when perfusion levels drop. Disentangling all of the different effects that occur under conditions of reduced perfusion is thus a substantial task, especially when attempting to interpret experimental data. This complexity is undoubtedly one of the key reasons why “the conclusions borne from theoretical studies have received little direct support from experiments”, Nilsson and Aalkjaer, 2003. The model that we present here thus attempts to shed additional insight onto this process by considering a previously neglected component, i.e. the non-linear interaction between the vessel wall movement and the dynamic concentration field in the surrounding tissue. We have neglected many other components of the problem, which will need to be examined in detail, together with the dynamic interaction considered here, to gain a full insight into the potentially key role of vasomotion in tissue protection. In particular, the non-linear dynamics of oxygen within tissue are likely to play a key role.

However, the results presented here do provide some interesting possibilities. For the typical values of Péclet number and non-dimensional rate constant calculated here, mass transport is reduced under nearly all conditions (except when the wall concentration oscillations are at a certain phase relative to the wall displacement oscillations, and even then the increase is very small). This reduction in the time-averaged mass transport between the oscillating and non-oscillating conditions appears rather surprising, given the discussion in the literature about vasomotion being a potential protective mechanism under conditions of ischemia. However, this process has to be considered within a complete network of vessels.

The behaviour of such a network in the context of vasomotion has previously been considered by, amongst others, Goldman et al., 2001, and Tsoukias et al., 2007. The former found that at physiological levels of tissue myoglobin vasomotion did not improve tissue oxygenation (but did so under other conditions). However, neither model considered the physical movement of the vessel walls as playing an important part in the tissue oxygenation process: only the flow field was oscillated and only the capillary bed was considered. This is similar to the work of Schneiderman et al., 1982, which examined the effects of oscillations in flow only. We have extended this work by considering the larger arteriolar vessels where vasomotion occurs, but have only considered a single vessel: more analysis will be required to investigate these vessels in a similar manner to these previous studies.

Oxygen delivery to tissue is found at both the arteriolar and capillary level, as shown by experimental data recorded by Vovenko, 1999, where the partial pressure of oxygen at inlet to the capillary bed was only of order 60 mmHg. The transport of oxygen to tissue thus occurs over a range of length scales, making interpreting the net effect of vasomotion highly complicated.

Vasomotive activity in the arteriolar bed appears to lead to a reduction in oxygen delivery to tissue: however, this ensures a greater oxygen concentration at entrance to the capillary bed. This would appear likely to promote oxygen transport within the capillary bed and thus could help to explain why vasomotion acts as a protective mechanism at the capillary level, rather than at the arteriolar level. It would then be seen as a means of retention of more oxygen for supply to the capillary bed.

If oscillations are present in the arteriolar vessel walls, this will also have the effect of perturbing the capillary flow field, both in terms of flow and concentration. It is not clear whether these oscillations will remain in significant amplitude at the capillary bed, since the arterial network acts as a low-pass filter to reduce the amplitude of flow oscillations (although significant oscillations in

red blood cell velocity have been observed experimentally in capillaries, Ellis et al., 2002), and, if they do, whether they would be sufficiently large to promote oxygen delivery in individual vessels in addition to the fact that the time-averaged oxygenation would also be higher. Much future work will be required to investigate the effects of this phenomenon across the vasculature.

In particular, the relationship between perturbations in the wall displacement and wall concentration will need to be determined. This could be done by solving the equations of motion and mass transport within the vessel and coupling them to the equations for wall displacement. Although this is relatively complicated, it would determine more definitely the nature of this coupling, which has been taken to be unknown here, and thus aid in interpreting the underlying physiological basis of vasomotion.

5 Conclusions

In this paper we have presented a technique for solving the non-linear mass transport equation for axisymmetric, axially invariant unbounded vessel-tissue systems with a periodically oscillating boundary. The results show that vasomotion alone causes the time-averaged mass transport to decrease under virtually all conditions, but that if the wall concentration oscillates in phase with this movement, then the time-averaged mass transport can increase under certain conditions. We therefore hypothesise that vasomotion might occur in the arteriolar network to decrease oxygen supply at this vascular level in order to increase the transport of oxygen to the capillary bed, which could have protective implications under conditions of reduced perfusion and thus explain why vasomotion plays a role under such conditions.

Acknowledgments

This work was supported by a grant from the Wellcome Trust for a Biomedical Vacation Scholarship for TH.

References

Bentley, T.B., Meng, H. and Pittman, R.N.(1993) Temperature dependence of oxygen diffusion and consumption in mammalian striated muscle. *Am. J. Physiol.*, 264: H1825-H1830.

Colantuoni, A., Bertuglia, S., and Intaglietta, M. (1984) Quantitation of rhythmic diameter changes in arterial microcirculation, *Am. J. Physiol.*, 246: H508-H517.

Ellis, C.G., Bateman, R.M., Sharpe, M.D., Sibbald, W.J. and Gill, R. (2002) Effect of a maldistribution of microvascular blood flow on capillary O₂ extraction in sepsis, *Am. J. Physiol.*, 282: H156-H164.

Fyrillas, M.M. and Szeri, A.J. (1994) Dissolution or growth of soluble spherical oscillating bubbles, *J. Fluid Mech.*, 277: 381-407.

Goldman, D. and Popel, A.S. (2001) A computational study of the effect of vasomotion on oxygen transport from capillary networks, *J. Theor. Biol.*, 209: 189-199.

Golub A.S., Barker, M.C. and Pittman, R.N. (2007) PO₂ profiles near arterioles and tissue oxygen consumption in rat mesentery, *Am. J. Physiol.*, 293: H1097-H1106.

Meyer, C., De Vries, G., Davidge, S.T. and Mayes, D.C. (2002) Reassessing the mathematical modelling of the contribution of vasomotion to vascular resistance, *J. Appl. Physiol.*, 92: 888-889.

Mintun, M.A., Lundstrom, B.N., Snyder, A.Z., Vlassenko, A.G., Shulman, G.L. and Raichle, M.E. (2001) Blood flow and oxygen delivery to human brain during functional activity: Theoretical modelling and experimental data, *PNAS* 98: 6859–6864.

Nilsson, H. and Aalkjaer, C. (2003) Vasomotion: Mechanisms and physiological importance, *Molecular Interventions*, 3: 79-89.

Rücker, M., Strobel, O., Vollmar, B., Roesken, F. and Menger, M.D. (2000) Vasomotion in critically perfused muscle protects adjacent tissues from capillary perfusion failure, *Am. J. Physiol.*, 279: H550-H558.

Schneiderman, G., Mockros, L.F. and Goldstick, T.K. (1982) Effect of pulsatility on oxygen transport to the human arterial wall. *J. Biomechanics*, 15: 849-858.

Sharan, M., Vovenko, E.P., Vadapalli, A., Popel, A.S. and Pittman, R.N. (2008) Experimental and theoretical studies of oxygen gradients in rat pial microvessels. *J. Cerebral Blood Flow and Metabolism*, 28: 1597-1604.

Tsai, A.G., Friesenecker, B., Mazzoni, M.C., Kerger, H., Buerk, D.G., Johnson, P.C. and Intaglietta, M. (1998) Microvascular and tissue oxygen gradients in the rat mesentery, *PNAS*. 95: 6590-6595.

Tsai, A.G. and Intaglietta, M. (1993) Evidence of flowmotion induced changes in local tissue oxygenation, *Int. J. Microcirc. Clin. Exp.*, 12: 75-88.

Tsoukias, N.M., Goldman, D., Vadapalli, A., Pittman, R.N. and Popel, A.S. (2007) A computational model of oxygen delivery by hemoglobin-based oxygen carriers in three-dimensional microvascular networks, *J. Theoretical Biology*, 248: 657-674.

Vovenko, E. (1999) Distribution of oxygen tension on the surface of arterioles, capillaries and venules of brain cortex and in tissue in normoxia: an experimental study on rats, *Eur. J. Physiol.*, 437: 617-623.

Figure Captions

Figure 1 - Typical model predictions for concentration profile components

Figure 2 - The effect of vasomotion on the rate of mass transport at different values of the Péclet number, at $K=1$

Figure 3 - The effect of vasomotion on the rate of mass transport at different values of the Péclet number, at $K=10$

Figure 4 - The effect of vasomotion on the rate of mass transport at different values of the Péclet number, at $K=0.1$

Figure 5 - The effect of vasomotion on the rate of mass transport at different values of the Péclet number, with concentration oscillating in phase with the wall

Figure 6 - The effect of vasomotion on the rate of mass transport at different values of the Péclet number, with concentration oscillating 90° in advance of the wall

Figure 7 - The effect of vasomotion on the rate of mass transport at different values of the Péclet number, with concentration oscillating 180° in advance of the wall

Figure 8 - The effect of vasomotion on the rate of mass transport at different values of the Péclet number, with concentration oscillating 270° in advance of the wall

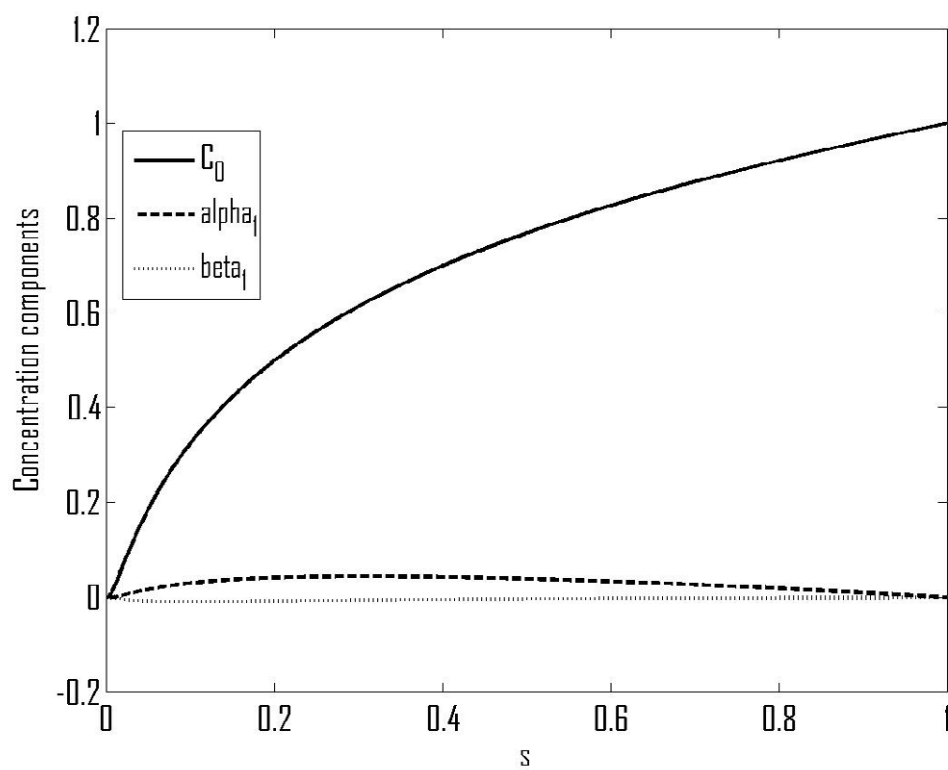


Figure 1 – Typical model predictions for concentration profile components.

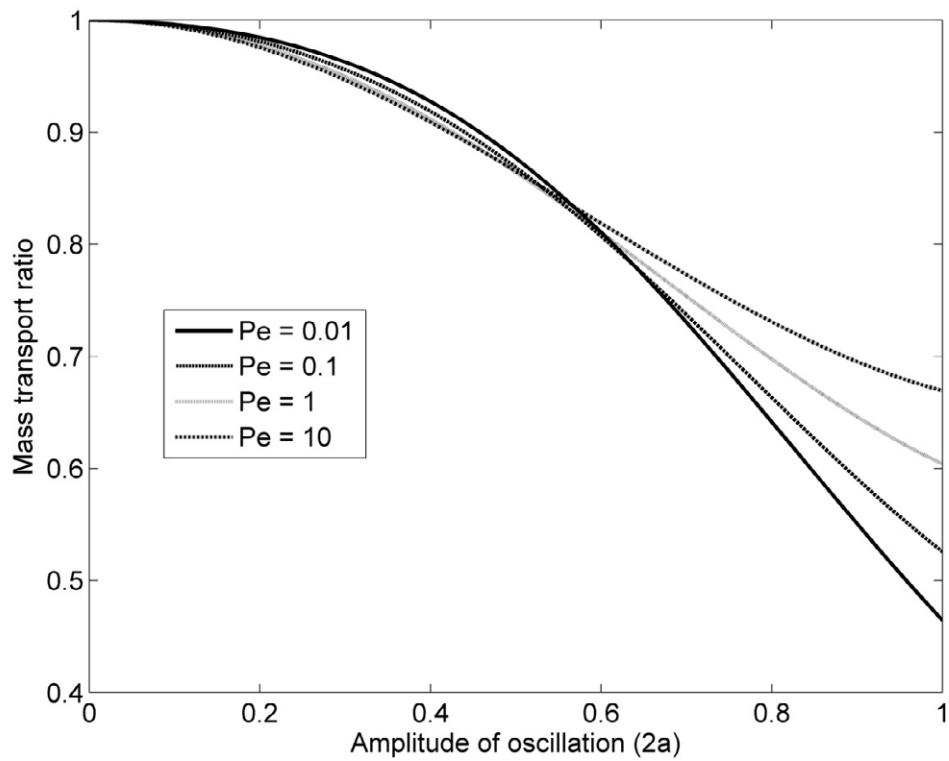


Figure 2 - The effect of vasomotion on the rate of mass transport at different values of the Péclet number, at $K=1$.

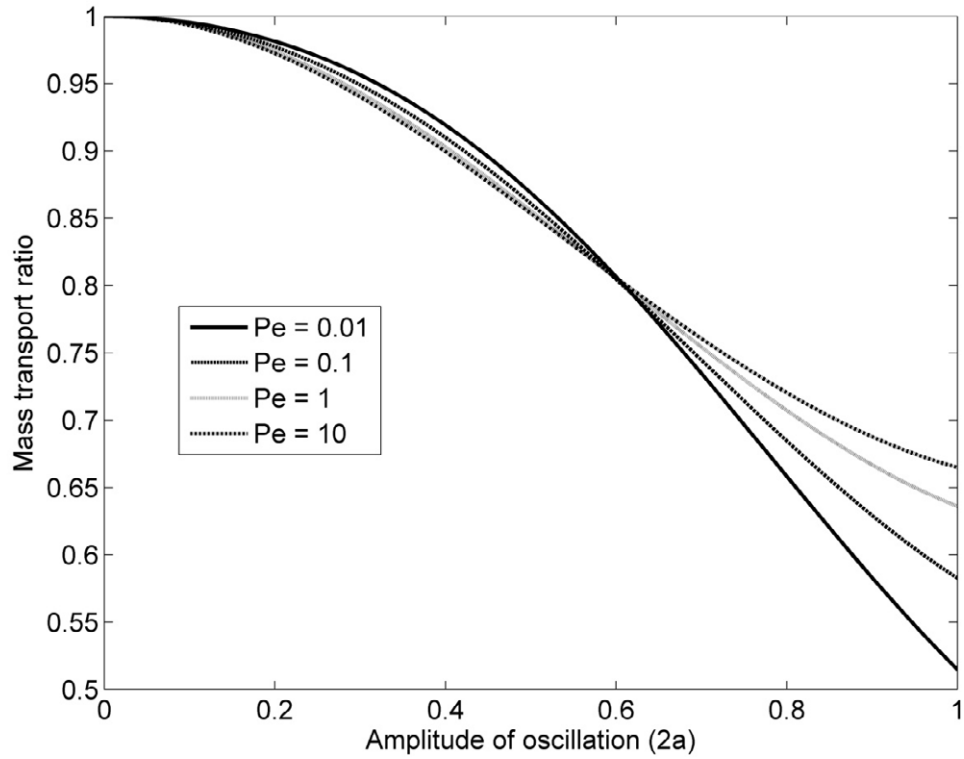


Figure 3 - The effect of vasomotion on the rate of mass transport at different values of the Péclet number, at $K=10$.

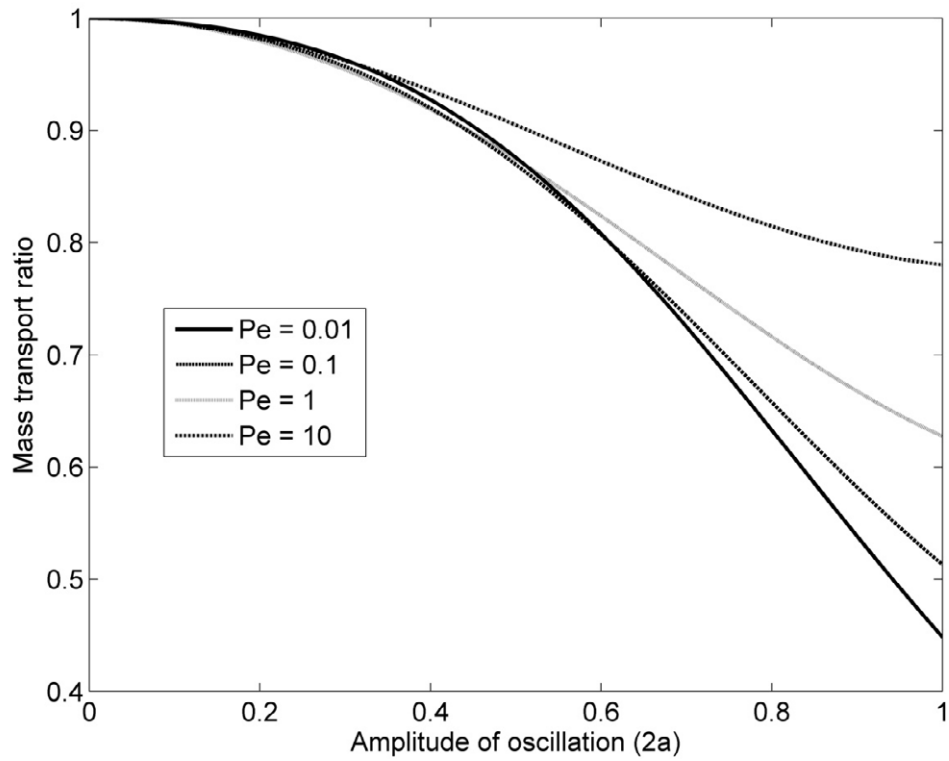


Figure 4 - The effect of vasomotion on the rate of mass transport at different values of the Péclet number, at $K=0.1$.

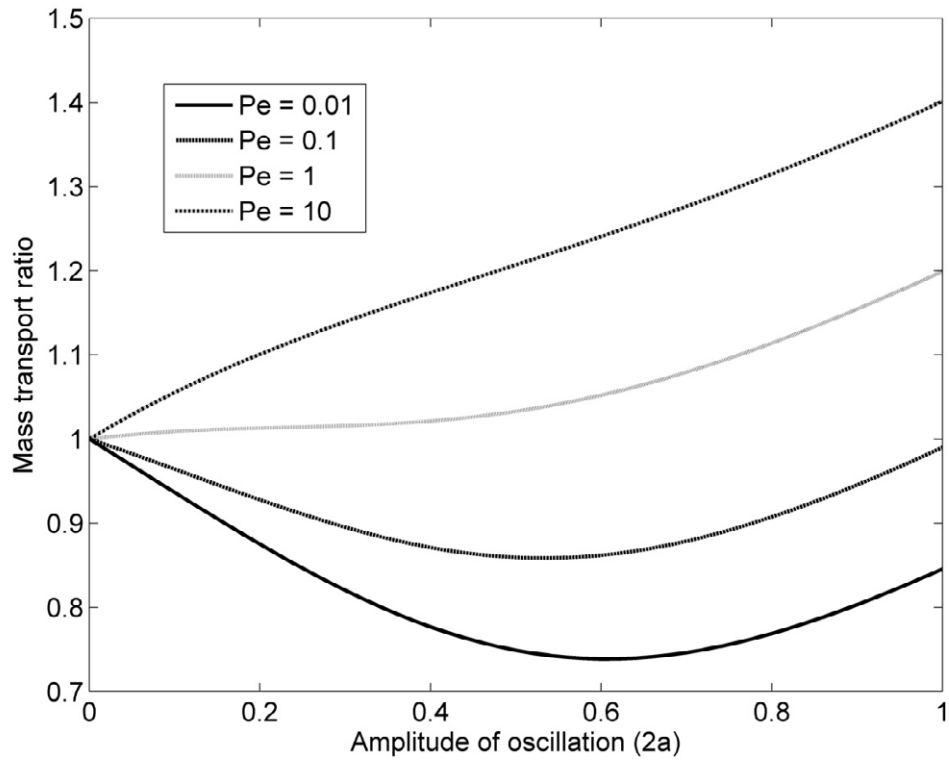


Figure 5 - The effect of vasomotion on the rate of mass transport at different values of the Péclet number, with concentration oscillating in phase with the wall.

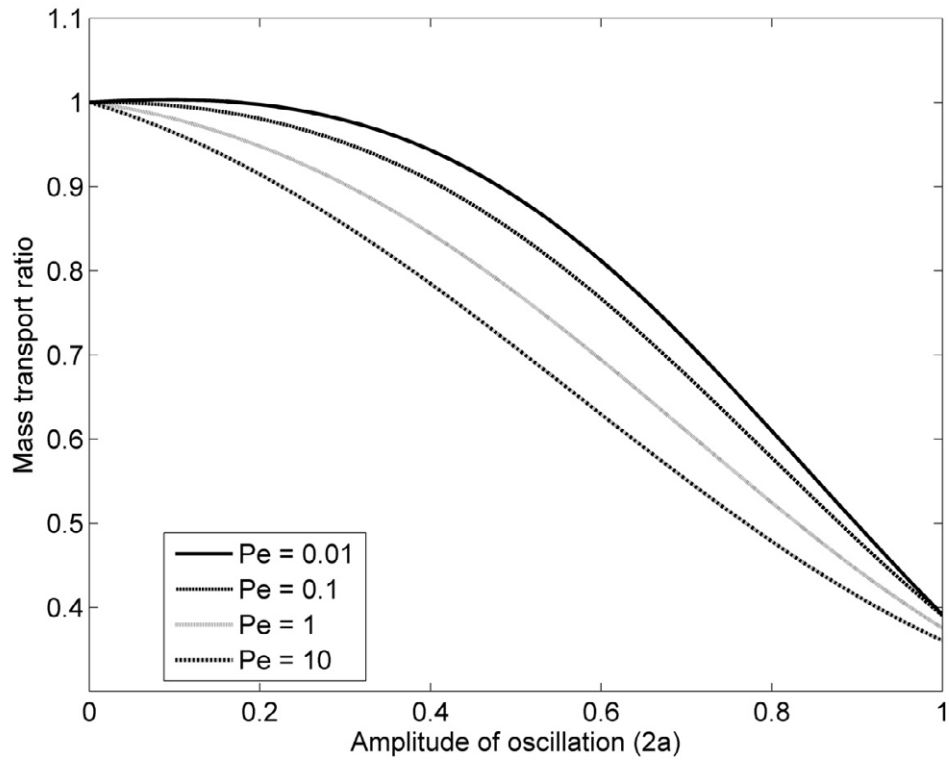


Figure 6 - The effect of vasomotion on the rate of mass transport at different values of the Péclet number, with concentration oscillating 90° in advance of the wall.

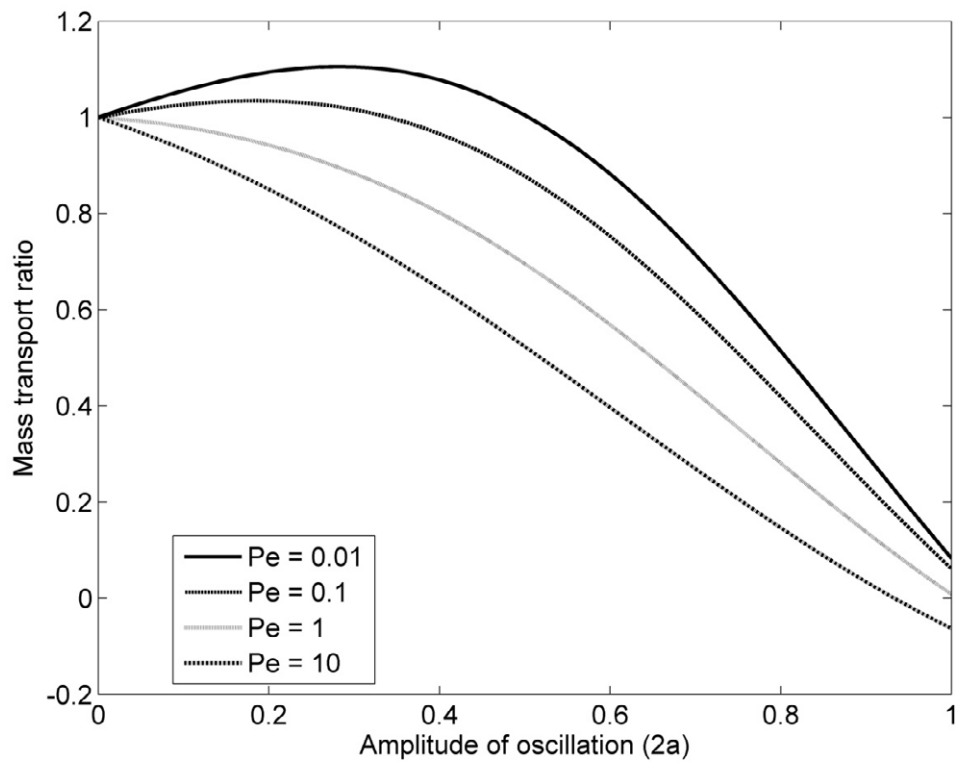


Figure 7 - The effect of vasomotion on the rate of mass transport at different values of the Péclet number, with concentration oscillating 180° in advance of the wall.

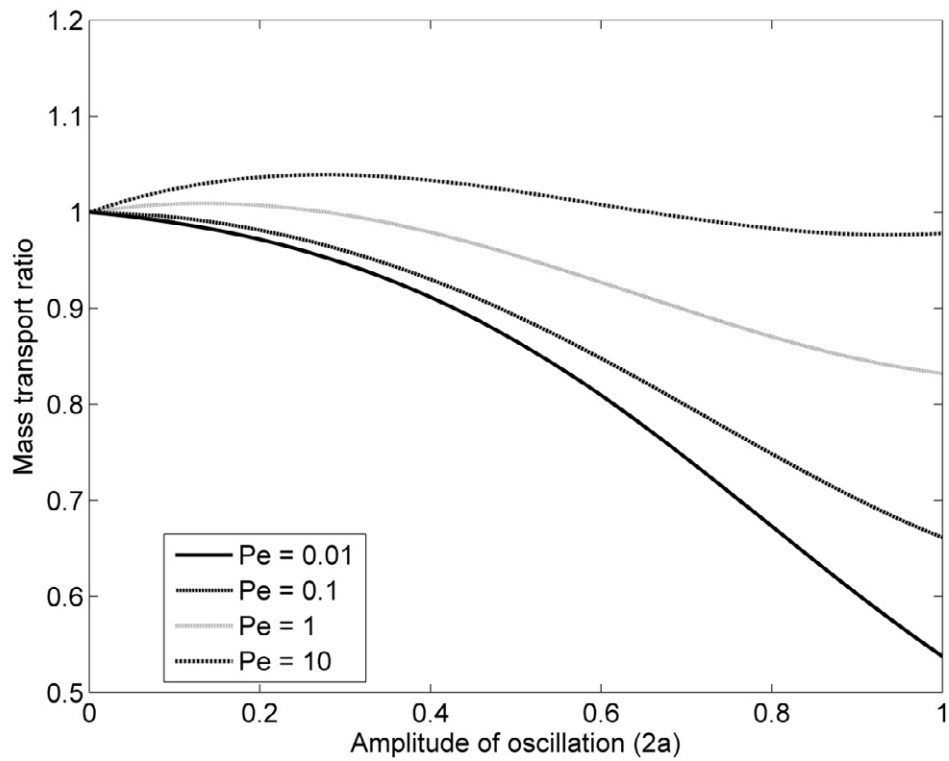


Figure 8 - The effect of vasomotion on the rate of mass transport at different values of the Péclet number, with concentration oscillating 270° in advance of the wall.